Journal of Statistical Physics, Vol. 92, Nos. 3/4, 1998

Electron Conductance and Lifetimes in a Ballistic Electron Waveguide

Kyungsun Na[1] and L. E. Reichl[1]

Received January 13, 1998; final May 12, 1998

Ballistic electron waveguides are open quantum systems that can be formed at very low temperatures at a GaAs/AlGaAs interface. Dissipation due to electron–phonon and electron–electron interactions in these systems is negligible. Although the electrons only interact with the walls of the waveguide, they can have a complicated spectrum including both positive energy bound states and quasibound states which appear as complex energy poles of the scattering S-matrix or energy Green's function. The quasibound states can give rise to zeros in the waveguide conductance as the energy of the electrons is varied. The width of the conduction zeros is determined by the lifetimes of the quasibound states. The "complex energy spectrum" associated with the quasibound states also governs the survival probability of electrons placed in the waveguide cavities.

KEY WORDS: Conductance; electron waveguide; electron scattering; Landauer formula.

I. INTRODUCTION

Electron waveguides can be formed at a GaAs/AlGaAs interface. In a typical experiment,[1,2] a two dimensional electron gas (2DEG) is located ~ 500 Å below the surface of the GaAs/AlGaAs heterostructure. Two dimensional leads and cavities of any shape, and of sizes ranging from 100 Å to 1000 Å, can be formed at the interface by depositing metal gates on the surface of the heterostructure and applying a negative voltage to the metal gates. This depletes the electrons in the part of the electron gas below the gates and confines the gas to the leads and cavities. The electron gas

[1] Center for Studies in Statistical Mechanics and Complex Systems, University of Texas at Austin, Austin, Texas 78712.

0022-4715/98/0800-0519$15.00/0

is two dimensional because only the lowest subband in the direction perpendicular to the plane of the interface is occupied and the higher subbands do not play any significant role. At temperatures of $T \sim 0.1 \rightarrow 2.0$ K, scattering events due to electron-phonon interactions have a mean free path, $L_{ph} \sim 30\,\mu$m.[3] Also, phase decoherence due to electron-electron scattering becomes negligible.[3] Therefore, at these low temperatures, the electrons travel through the leads and cavities ballistically and scattering comes only from the sample boundaries since the scattering with impurities can be neglected.

There have been a number of studies of the ballistic electron transport in quantum waveguides of different shapes. These studies have been variously concerned with conductance quantization and with the relation between the shape of the waveguide and the existence of bound and quasibound states. References 4 and 5, for example, deal with waveguides with curved leads. References 6–10 deal with waveguides with straight leads but of cavities with different shapes. In this paper, we restrict ourselves to waveguides with rectangular cavities which are connected to electron reservoirs by long straight leads. Such systems have also been studied by Okiji, Kasai, and Nakamura[6] who focused on conductance quantization as a function of energy, on varying the confinement dimensions, and varying the applied magnetic field using a wavefunction matching method. Berggren and Ji[7] studied resonant tunneling due to the presence of bound states in rectangular waveguide stuctures with very short lead lengths, also using a wavefunction matching method. Itoh, Sano, and Yoshii[8] used a tight-binding Green's function method to study the effect of quasi-bound states on conduction and the density of states. Lent[9] and Lent and Sivaprakasam[11] examined the conductance properties of waveguides with rectangular cavities but focused on cavity current vortex excitations in these devices. In this paper, we are interested primarily in the spectral properties of waveguides with rectangular cavities, and the effect of the spectrum on the waveguide conductance and electron dwell times in the cavity. We assume that the electrons in the waveguide are in thermal equilibrium. At the very low temperatures we will consider, the electrons are distributed according to the Fermi-Dirac distribution.

For systems of the above type, the conductance is believed to be related to the scattering transmission probability by the Landauer–Buttiker formula. In this paper, we will sketch the derivation of the Landauer–Buttiker formula[12] from linear response theory for the particular waveguide we are interested in. We will also relate the conductance to the energy Green's function for the waveguide and through numerical calculations show the implications of these theories for the conductance of the waveguide and on the survival probabilities of electrons in the waveguide.

In Section II, we describe our waveguide and derive the Landauer–Buttiker formula for it. In Section III, we give a short summary of the method we use to calculate the energy eigenstates used to compute the conductance and survival probabilities. In Section IV we show our numerical results for the conductivity of the waveguide. In Section V, we compute electron survival probabilities in the waveguide. In Section VI, we conclude.

II. THEORY

We shall consider the simple waveguide shown in Fig. 1 which consists of a rectangular cavity to which two leads are attached. The walls of the cavity and leads are infinitely hard and the leads are infinitely long. The leads have a width, $W = 100$ Å. The cavity has a length, $L = 371.66$ Å and a width, D, which we shall vary. The electrons propagate along the x-direction and set up standing waves along the y-direction. The Fermi energy of the two dimensional electron gas in the waveguide is $E_f = \pi n_e h^2/m$, where h is Planck's constant, n_e is the density of electrons, and m is the effective mass of the electrons. Both n_e and m depend on the materials used to construct the 2DEG. We will use a generic effective mass, $m = 0.05m_e$, where m_e is the mass of the free electron (for GaAs, $m = 0.067m_e$). When the electron density is $n_e = 4.0 \times 10^{12}\ \text{cm}^{-2}$, for example, the Fermi energy is $E_f = 0.192$ eV.

The conductivity tensor can be found from linear response theory.[13–15] We here adapt that theory to our waveguide. We write the electron Hamiltonian in the form, $\hat{H}(t) = \hat{H} + \delta\hat{H}(t)$, where $\hat{H} = \hat{\mathbf{p}}^2/2m + \hat{V}_{wall}(\hat{\mathbf{q}})$, $\delta\hat{H}(t)$ is a weak perturbation, and $\hat{\mathbf{p}}$ and $\hat{\mathbf{q}}$ are the electron momentum and position operators. The potential, $\hat{V}_{wall}(\hat{\mathbf{q}})$ contains all information about the shape of the walls. We will choose $\delta\hat{H}(t) = eV(x)\,\Theta(t)$, where $V(x)$ is a weak localized electric potential pulse and $\Theta(t)$ is a finite time envelope over which the potential pulse is applied.

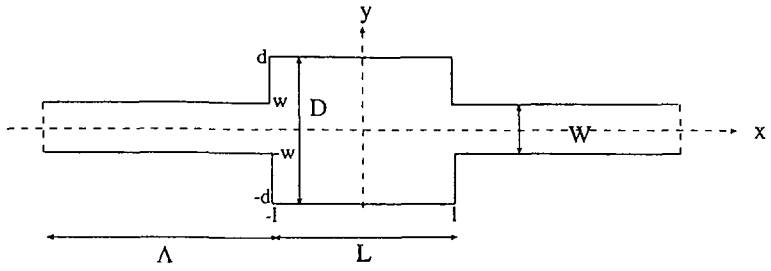

Fig. 1. Geometry of the waveguide.

The density operator for the electron state can be written, $\hat{\rho}(t) = \hat{\rho}_{eq} + \delta\hat{\rho}(t)$, where $\hat{\rho}_{eq}$ is the equilibrium density operator, $\hat{\rho}_{eq} = \exp(-\hat{H}/k_B T)$, k_B is Boltzmann's constant, and T is temperature in Kelvin. The quantity, $\delta\hat{\rho}(t)$, is the correction to the equilibrium density operator due to the perturbation, $\delta\hat{H}(t)$. The equation of motion of the density operator is $i\hbar(\partial\hat{\rho}(t)/\partial t) = [\hat{H}(t), \hat{\rho}(t)]$. To lowest order in $\delta\hat{H}(t)$,

$$\delta\hat{\rho}(t) = \frac{1}{i\hbar}\int_{-\infty}^{t} dt' [e^{-i\hat{H}_0(t-t')/\hbar}\,\delta\hat{H}(t')\,e^{+i\hat{H}_0(t-t')/\hbar}, \hat{\rho}_{eq}] \tag{2.1}$$

The electric current operator, at point $\mathbf{r}$ in the waveguide is $\hat{\mathbf{J}}(\mathbf{r}) = (e/2m)(\hat{\mathbf{p}}\delta(\hat{\mathbf{q}}-\mathbf{r}) + \delta(\hat{\mathbf{q}}-\mathbf{r})\hat{\mathbf{p}})$. The perturbation induces an average current $\langle \mathbf{J}(\mathbf{r}, t)\rangle = \mathrm{Tr}[\hat{\mathbf{J}}(\mathbf{r})\,\delta\hat{\rho}(t)]$. We will evaluate the trace using complete sets of energy eigenstates, $|E_\alpha\rangle$, of the Hamiltonian, $\hat{H}$. The index, α ranges over all possible states and will have discrete and continuous parts. In most cases, we must obtain these states numerically. The equilibrium density operator can be written, $\rho_{eq} = \sum_\alpha f(E_\alpha)\,|E_\alpha\rangle\langle E_\alpha|$, where $f(E_\alpha) = (\exp[\beta(E_\alpha - \mu)] + 1)^{-1}$ is the equilibrium Fermi-Dirac distribution for the two dimensional electron gas and μ is the chemical potential. Matrix elements of the current are $\mathbf{J}_{\alpha\beta}(\mathbf{r}) = -(ie\hbar/2m)[\psi_\alpha^*(\mathbf{r})\,\nabla_{\mathbf{r}}\psi_\beta(\mathbf{r}) - (\nabla_{\mathbf{r}}\psi_\alpha(\mathbf{r}))^*\,\psi_\beta(\mathbf{r})]$, where $\psi_\alpha(\mathbf{r}) = \langle \mathbf{r} \mid E_\alpha\rangle$ and $|\mathbf{r}\rangle$ is the eigenket of $\hat{\mathbf{q}}$. If we assume that $V(x = \pm\infty, t) = 0$, then the perturbation can be written in the form $\delta\hat{H}_{\beta\alpha}(t) = (-i\hbar/(E_\alpha - E_\beta))$ $\int d\mathbf{r}\,\mathbf{J}_{\beta\alpha}(\mathbf{r})\cdot\mathbf{E}(\mathbf{r}, t)$, where $\mathbf{E}(\mathbf{r}, t) = E(x)\,\Theta(t)\,\hat{\mathbf{i}}$, $E(x) = -dV(x)/dx$ is the applied electric field, and $\hat{\mathbf{i}}$ is a unit vector in the x-direction.

For this system, the average current only flows along the x-axis so we only need to find the average of the x-component of the current, which takes the form

$$\langle J_x(\mathbf{r}, t)\rangle = \int_{-\infty}^{\infty} dt' \int d\mathbf{r}'\,\sigma_{xx}(\mathbf{r}, \mathbf{r}'; t-t')\,E(x')\,\Theta(t') \tag{2.2}$$

where $\sigma_{xx}(\mathbf{r}, \mathbf{r}'; t-t')$ is the xx-element of the conductivity tensor and is given by

$$\sigma_{xx}(\mathbf{r}, \mathbf{r}'; t-t') = -\sum_\alpha \sum_\beta \frac{(f_\alpha - f_\beta)}{(E_\alpha - E_\beta)} J_{x;\,\alpha\beta}(\mathbf{r})\,e^{-i(E_\alpha - E_\beta)(t-t')/\hbar} J_{x;\,\beta\alpha}(\mathbf{r}')\,\theta(t-t') \tag{2.3}$$

$\theta(t-t')$ is the Heaviside function ($\theta(t) = 1$ for $t > 0$ and $\theta(t) = 0$ for $t < 0$) and $J_{x;\,\alpha\beta}$ is the x-component of the current matrix element. The conductivity is a response function and must satisfy causality, $\sigma_{xx}(\mathbf{r}, \mathbf{r}'; t-t') = 0$ for $t - t' < 0$, and the response must be finite so $\int_0^\infty dt\,\sigma_{xx}(\mathbf{r}, \mathbf{r}'; t) < \infty$.

The total power, P_{tot}, absorbed by the waveguide is

$$P_{tot} = \int_{-\infty}^{\infty} \frac{d\omega}{2\pi} \int d\mathbf{r} \int d\mathbf{r}'\, E(x)\, \tilde{\Theta}(-\omega)\, \tilde{\sigma}_{xx}(\mathbf{r}, \mathbf{r}'; \omega)\, E(x')\, \tilde{\Theta}(\omega) \tag{2.4}$$

where $\tilde{\Theta}(\omega) = \int_{-\infty}^{\infty} dt\, e^{i\omega t}\Theta(t)$ and

$$\begin{aligned} \tilde{\sigma}_{xx}(\mathbf{r}, \mathbf{r}'; \omega) &= \lim_{\delta \to 0} \int_{-\infty}^{\infty} dt\, e^{i(\omega + i\delta)t} \sigma_{xx}(\mathbf{r}, \mathbf{r}'; t) \\ &= -i \lim_{\delta \to 0} \sum_{\alpha} \sum_{\beta} \frac{(f_\alpha - f_\beta)}{(E_\alpha - E_\beta)} \frac{J_{x;\alpha\beta}(\mathbf{r})\, J_{x;\beta\alpha}(\mathbf{r}')}{(\omega - (E_\alpha - E_\beta)/\hbar + i\delta)} \end{aligned} \tag{2.5}$$

This in turn leads to the result

$$P_{tot} = \int_{-\infty}^{\infty} \frac{d\omega}{2\pi} \int d\mathbf{r} \int d\mathbf{r}'\, E(x)\, \tilde{\Theta}(-\omega)\, \mathrm{Re}\, \tilde{\sigma}_{xx}(\mathbf{r}, \mathbf{r}'; \omega)\, E(x')\, \tilde{\Theta}(\omega) \tag{2.6}$$

Thus, the real part of the conductivity,

$$\mathrm{Re}\, \tilde{\sigma}_{xx}(\mathbf{r}, \mathbf{r}'; \omega) = -\sum_{\alpha} \sum_{\beta} \frac{(f_\alpha - f_\beta)}{(E_\alpha - E_\beta)} J_{x;\alpha\beta}(\mathbf{r})\, J_{x;\beta\alpha}(\mathbf{r}')\, \delta(\omega - (E_\alpha - E_\beta)/\hbar) \tag{2.7}$$

is dissipative and determines the conductance of the wave guide.

Because the leads are straight, the spatial degrees of freedom in the leads are uncoupled. The energy eigenstates in the leads have the form, $\psi_{kn}(x, y) = \phi_{kn}(x)\, \chi_n(y)$, where $\chi_n(y) = \sqrt{2/W}\, \sin(n\pi y/W)$ is the transverse part of the nth propagating mode, and $\phi_{kn}(x)$ must be found numerically. The energy eigenvalue of this state is $E_{kn} = \hbar^2/2m[k^2 + (n\pi/W)^2]$. For our waveguide with $W = 100$ Å, only a single mode ($n = 1$) can propagate in the leads for Fermi energies between $E_F = \hbar^2/2m(\pi/W)^2 = 0.075$ eV and $E_F = \hbar^2/2m(2\pi/W)^2 = 0.302$ eV. This is the energy regime we will be most interested in.

Let us assume the cavity lies between $x = -L/2$ and $x = L/2$. We apply the perturbation, $E(x)$, to the left of the cavity and find the current to the right of the cavity. Thus we are interested in the conductivity, $\mathrm{Re}\, \tilde{\sigma}_{xx}(x_R, y, x_L, y'; \omega)$, where $x_R > L/2$ and $x_L < -L/2$. The current for values of x outside the cavity is given by $J_{x,y;k'n',kn}(x, y) = J_{x;k'n',kn}(x)\, \chi_{n'}(y)\, \chi_n(y)$ where $J_{x;k'n',kn}(x) = -ie\hbar/2m[\phi^*_{k'n'}(x)\, (d\phi_{kn}(x)/dx) - (d\phi^*_{k'n'}(x)/dx)\, \phi_{kn}(x)]$. When the conductivity is evaluated at points outside the cavity, the contribution from the transverse modes decouples

and can be integrated out. If we define $\tilde{\sigma}_{xx}(x_R, x_L; \omega) = \int_{-w}^{w} dy \times \int_{-w}^{w} dy' \, \tilde{\sigma}_{xx}(x_R, y, x_L, y'; \omega)$ and take the limit $\omega \to 0$ and the limit $T \to 0$ K, we obtain for the static conductivity

$$\operatorname{Re} \tilde{\sigma}_{xx}(x_R, x_L; 0) = \hbar \sum_{n=1}^{n_c} \int_{-\infty}^{\infty} dk \int_{-\infty}^{\infty} dk' \, J_{x_R;\, k'n,\, kn}(x) \times J_{x_L;\, kn,\, k'n}(x) \, \delta(E_F - E_{k'n}) \, \delta(E_F - E_{kn}) \tag{2.8}$$

where n_c is the quantum number for the highest allowed propagating mode.

Fisher and Lee[14] showed that the static conductivity could be written in terms of the retarded, G_E^+, and advanced, G_E^-, energy Green's functions, where $G_E^{\pm} = (E - \hat{H} \pm i\delta)^{-1}$. If we restrict ourselves to Fermi energies which allow only one propagating mode in the leads so $n_c = 1$, the Green's functions in the leads can be written, $G_E^{\pm}(x_R, y, x_L, y') = g_E^{\pm}(x_R, x_L) \chi_1(y) \chi_1(y')$, where

$$g_E^{\pm}(x_R, x_L) = \int_{-\infty}^{\infty} dk \, \frac{\phi_{k1}^*(x_R) \, \phi_{k1}(x_L)}{E - E_{k1} \pm i\delta} \tag{2.9}$$

Fisher and Lee[14] showed that

$$\operatorname{Re} \tilde{\sigma}_{xx}(x_R, x_L; 0) = -\frac{\hbar}{\pi} \left(\frac{e\hbar}{2m} \right)^2 k_{F,1}^2 [\, g_{E_F}^+(x_R, x_L) \, g_{E_F}^+(x_L, x_R) + g_{E_F}^-(x_R, x_L) \, g_{E_F}^-(x_L, x_R)] \tag{2.10}$$

By using Green's theorem, the Green's function can be related to the scattering transmission amplitude, T_{11}, for the single propagating mode in the waveguide incident from the left[14, 16] so

$$T_{11}(E_F) = \frac{i\hbar^2 k_{F,1}}{m} e^{ik_{F,1}(x_R - x_L)} g_{E_F}^+(x_L, x_R) \tag{2.11}$$

With this relation the static conductivity becomes

$$\operatorname{Re} \tilde{\sigma}_{xx}(x_R, x_L; 0) = \frac{e^2}{h} |T_{11}|^2 \tag{2.12}$$

This is the Landauer–Buttiker formula relating static conductance to the scattering transmission probability. Eq. (2.11) relates the energy Green's function to the transmission amplitude. In the subsequent sections we will explore the implications of these relations for our waveguide.

III. METHOD FOR OBTAINING ENERGY EIGENSTATES

Our calculations of the exact energy eigenstates, $\psi_{kn}(x, y)$, were done using the boundary integral method developed by Frohne, McLennan, and Datta.[17] The exact eigenstates, $\psi_{kn}(x, y)$, are built out of local propagating and evanescent modes in the leads and cavity. The electron enters the cavity from the left in a pure propagating mode, n_o. The energy eigenstates in the left and right leads, respectively, can be written,

$$\Psi_L(x, y) = \frac{1}{\sqrt{k_{n_o}}} e^{ik_{n_o}(x+l)}\chi_{n_o}(y) + \sum_{n=1}^{\infty} R_{nn_o} c_n e^{-ik_n(x+l)}\chi_n(y) \qquad \text{for} \quad x < -l \tag{3.1}$$

and

$$\Psi_R(x, y) = \sum_{n=1}^{\infty} T_{nn_o} c_n e^{ik_n(x-l)}\chi_n(y) \qquad \text{for} \quad x > l \tag{3.2}$$

where $l = L/2$. The summation index, n, *for this section of the paper only*, contains both propagating and evanescent modes. For propagating modes, $1 \leqslant n \leqslant n_c$, where n_c is the quantum number of the highest propagating mode. For evanescent modes, $n_c < n$. For propagating modes, $c_n = 1/\sqrt{k_n}$ and k_n is real. For evanescent modes $c_n = \sqrt{2}$ and $k_n = i\kappa_n$. The transverse contribution to the wave function, $\chi_n(y)$, is given by

$$\chi_n(y) = \begin{cases} \sqrt{\dfrac{1}{w}} \cos\left(\dfrac{n\pi y}{2w}\right), & \text{if} \quad n = 1, 3, 5, \ldots \\ \sqrt{\dfrac{1}{w}} \sin\left(\dfrac{n\pi y}{2w}\right), & \text{if} \quad n = 2, 4, 6, \ldots \end{cases} \tag{3.3}$$

The coefficients, R_{nn_o} and T_{nn_o}, are the reflection and transmission probability amplitudes, respectively. Each propagating mode carries unit current since it is normalized with the factor, $1/\sqrt{k_n}$. For the evanescent mode, $\sqrt{2}$ comes from the normalization of the longitudinal part of the wave function in the lead. Conservation of probability requires that $\sum_{n=1}^{n_c} \sum_{n_o=1}^{n_c} (|R_{nn_o}|^2 + |T_{nn_o}|^2) = n_c$.

The wavefunction for the electrons inside the cavity can be written

$$\Psi_C(x, y) = \sum_{n'=1}^{\infty} d_{n'}(C_{n'n_o} e^{ik_{n'}x} + C'_{n'n_o} e^{-ik_{n'}x})\chi_{n'}(y) \qquad \text{for} \quad -l < x < l \tag{3.4}$$

where $C_{n'n_0}$ and $C'_{n'n_0}$ are probability amplitudes of the wavefunctions inside the cavity. The normalization constant for propagating modes, $d_{n'} = \sqrt{1/2l}$ and for evanescent modes, $d_{n'} = \sqrt{2k_{n'}e^{2k_{n'}l}/(e^{4k_{n'}l} - 1)}$. The transverse part of the n'th mode, $\chi_{n'}(y)$, is given by

$$\chi_{n'}(y) = \begin{cases} \sqrt{\frac{1}{d}} \cos\left(\frac{n'\pi y}{2d}\right), & \text{if } n' = 1, 3, 5,... \\ \sqrt{\frac{1}{d}} \sin\left(\frac{n'\pi y}{2d}\right), & \text{if } n' = 2, 4, 6,... \end{cases} \tag{3.5}$$

The energy of the n^{th} mode in the leads is given by $E^{lead} = (\hbar^2/2m) \times (k_n^2 + (n\pi/W)^2)$. The energy of the n'th mode in the cavity is given by $E^{cavity} = (\hbar^2/2m)(k_{n'}^2 + (n'\pi/D)^2)$. For a given Fermi energy, there can be both propagating modes (real wavevectors) and evanescent modes (pure imaginary wavevectors).

The cavity we consider (Fig. 1) has hard walls at $y = \pm d$. It also has vertical hard wall segments at $x = \pm l$. Along the vertical hard wall segments, the wave function, $\Psi_{R,L}(x, y)$, vanishes but the normal derivative of $\Psi_{R,L}(x, y)$ along the hard wall segments does not vanish. Therefore we need wavefunctions outside the vertical hard wall segments to match the normal derivatives of the wavefunctions inside the cavity at the wall. We write

$$\frac{\partial \Psi_{R,L}}{\partial \hat{n}}(x, y) = \begin{cases} \sum_{n'} B_{n'n_0} b_{n'} e^{i2\pi n'(y+w)/d_1}, & \text{if } y < -w \\ \sum_{n'} B_{n'n_0} b_{n'} e^{i2\pi n'(y-w)/d_1}, & \text{if } y > w \end{cases} \tag{3.6}$$

where $b_n = \sqrt{1/d_1}$ and d_1 is the length of the segment of the hard wall considered. The wavefunction is normalized in that segment of the wall. The derivative with respect to $\hat{n}$ means outward normal direction at the wall.

Using the boundary integral method, the set of coefficients T_{nn_0}, R_{nn_0}, $C_{n'n_0}$ and $C'_{n'n_0}$ can be calculated (see Appendix). From $C_{n'n_0}$ and $C'_{n'n_0}$ we can obtain the wavefunction, $\Psi_C(x, y)$, inside cavity, and with it we can calculate the probability density of the electron, the electron current flux, and the total charge inside the cavity. The current inside the cavity is given by,

$$\mathbf{j} = \frac{eih}{2m^*}(\Psi_C(x, y) \nabla \Psi_C^*(x, y) - \Psi_C^*(x, y) \nabla \Psi_C(x, y)) \tag{3.7}$$

If we integrate the probability density over the whole cavity, we obtain a quantity which is,[11]

$$Q = \int_{cavity} |\Psi_C(x, y)|^2 \, dx \, dy \tag{3.8}$$

In Section V, we will compute the survival probabilities for electrons placed in the waveguide cavities using energy eigenstates of a closed version of the waveguide. We close the far ends of the very long leads and use the boundary integral method to compute the energy eigenstates of this now closed system. The eigenfunctions in left and right closed 'leads' can be constructed as follows.

$$\Psi_L(x, y) = \sum_{n=1}^{n_c} R_{nn_o} c_n \sin(k_n(x + l + \Lambda)) \chi_n(y) + \sum_{n=n_c+1}^{\infty} R_{nn_o} c_n' e^{k_n(x+l)} \chi_n(y) \qquad \text{for} \quad x < -l \tag{3.9}$$

and

$$\Psi_R(x, y) = \sum_{n=1}^{n_c} T_{nn_o} c_n \sin(k_n(x - l - \Lambda)) \chi_n(y) + \sum_{n=n_c+1}^{\infty} R_{nn_o} c_n' e^{-k_n(x-l)} \chi_n(y) \qquad \text{for} \quad x > l \tag{3.10}$$

where Λ is the length of the closed leads. For propagating modes, $c_n = \sqrt{4k_n/(2k_n\Lambda - \sin(2k_n\Lambda))}$ and k_n is real. For evanescent modes $c_n' = \sqrt{2k_n/(1 - e^{-2k_n\Lambda})}$ and $k_n = i\kappa_n$. The transverse contribution to the wave function, $\chi_n(y)$, is same as given by Eq. (3.3). It is easy to see that the wavefunction for the propagating mode vanishes at the lead ends ($x = -\Lambda - l$ and $x = \Lambda + l$). We then follow the same procedure as for the open system, except that there is no input mode. In this way, we obtain the eigenvalues and eigenstates of the closed waveguide. The energy eigenvalues for the closed system will be real and discrete. For very long leads the energy levels will be closely spaced and will allow us to mimic the continuous spectrum of the open system for a short time. We must make the energy level spacing small enough to observe the behavior of the open system that we are interested in. As we shall see, this can be done.

IV. THE CONDUCTANCE

We have computed the transmission probability, $|T_{11}|^2$, for the lowest propagating mode in the waveguide as a function of Fermi energy, for several different cavity widths. In the section below, we show the connection between singularities of $T_{11}(E)$ in the complex energy plane and the conductance.

IV.1. Transmission Zeros

In Fig. 2, we show the transmission probability, $|T_{11}|^2$, versus Fermi energy for several different cavity widths, D. In this waveguide, parity is conserved, so only those transverse modes inside the cavity with n' odd ($n' = 1, 3, 5,...$) can be excited by the incoming electron. As a function of Fermi energy, the transmission probability has a series of transmission zeros and each transmission zero has a width which varies from one transmission zero to the next. These transmission zeros have been seen before in

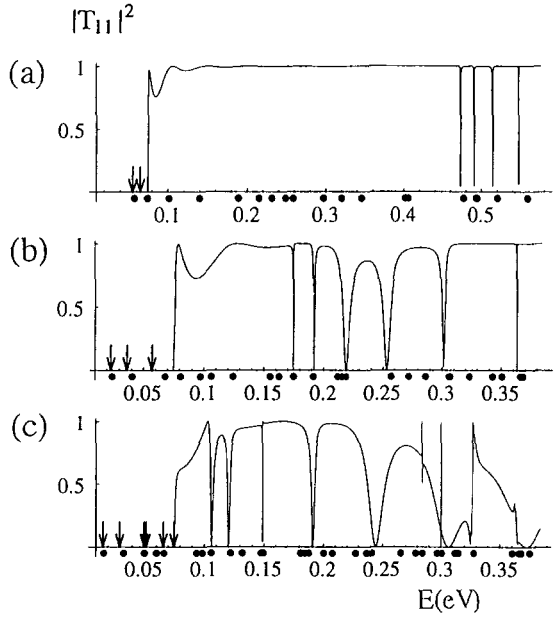

Fig. 2. Transmission probability, $|T_{11}|^2$, versus energy, E, for the straight waveguide with $W = 100$ Å, $L = 371.66$ Å, and (a) $D = 120$ Å, (b) $D = 200$ Å, and (c) $D = 260$ Å. The dark circles below the energy axis are all the eigenenergies of the closed cavity. The arrows indicate the positions of the bound states below the first channel.

numerical experiments[4–10] and perhaps in a laboratory experiment.[18] (We have also seen them when we fix the energy and vary the cavity length.)

Transmission zeros in a given channel have been related to Fano type resonances between the continuum of that channel and bound states of the closed cavity.[22, 23] The strength of the coupling between the continuum state and the bound state determines the decay rate and the width of the transmission profile.[5, 8, 19] Open systems with attractive weak potential,[20] quantum waveguides with impurities,[21] and bent quantum wires show similar phenomena.[4, 5]

Fig. 2(a) shows the transmission probability, $|T_{11}|^2$ (the solid line), for the cavity width, $D = 120$ Å. For energies, $0.075\text{ eV} < E < 0.302\text{ eV}$, only one propagating mode (one channel) in the leads is allowed and $|T_{11}|^2 = (h/e^2)G$, where G is the conductance. For the energy range $0.302\text{ eV} < E < 0.678\text{ eV}$ two propagating modes (two channels) exist in the lead. (For two propagating modes the static conductance is given by: $\tilde{\sigma}(x_R, x_L; \omega) = e^2/h(|T_{11}^2 + |T_{12}|^2 + |T_{21}|^2 + |T_{22}|^2)$.) There is only a small modulation in $|T_{11}|^2$ at lower energies. The first transmission zero occurs at an energy $E_F > 0.302$ eV. Due to the symmetry between the leads and the cavity, cavity bound states with transverse quantum number $n' = 2$ cannot couple to the continuum of the first channel and no bound states with transverse quantum number $n' = 3$ exist for $E_F < 0.302$ eV. Therefore, no transmission zeros occur at these lower energies. In Figs. 2(b) and 2(c) the cavity widths are $D = 200$ Å and $D = 260$ Å, respectively. We see that the transmission zeros now can occur when a single propagating mode (channel) exists in the leads because cavity bound states with transverse quantum number $n' = 3$ now lie in this energy range.

For the remainder of this paper, we will focus on the first three transmission zeros in Fig. 2(b). They can be linked to poles of $T_{11}(E)$ in the complex energy plane. To find the poles of $T_{11}(E)$, we first rewrite the wave function as a function of the complex energy, $E_R - iE_I$, and then match the wavefunction and the derivative of the wave function at the interfaces between the leads and the cavity using the method described in Section III. The transmission amplitude, $T_{11}(E)$, is a function of $\sqrt{E}$. It has a branch cut starting from the lower edge of the continuum and extending along the positive energy axis, and it has poles at energy values $E_R - i\gamma$. These poles give rise to the transmission zeros on the positive real axis.[21, 22]

Our plots in Fig. 3, show the transmission probability in the complex energy plane in the neighborhoods of the first three transmission zeros in Fig. 2(b). They show poles in the complex plane accompanied by zeros on the real energy axis. We shall refer to these structures as "pole-zero pairs." The distance between a pole and the real axis corresponds to the half width

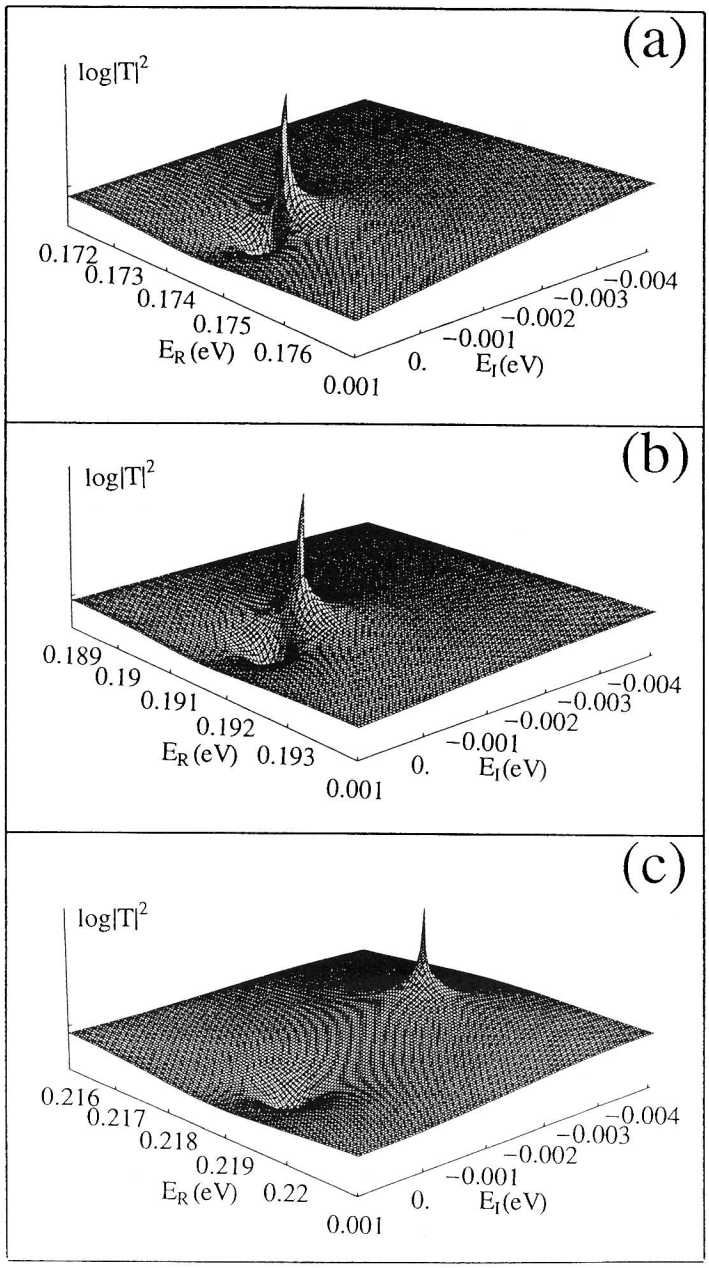

Fig. 3. 3D plots of the pole-zero pairs in the complex energy plane of the S-matrix for $D = 200$ Å near resonances (a) $E = 0.17487$ eV, (b) $E = 0.19196$ eV, and (c) $E = 0.21836$ eV.

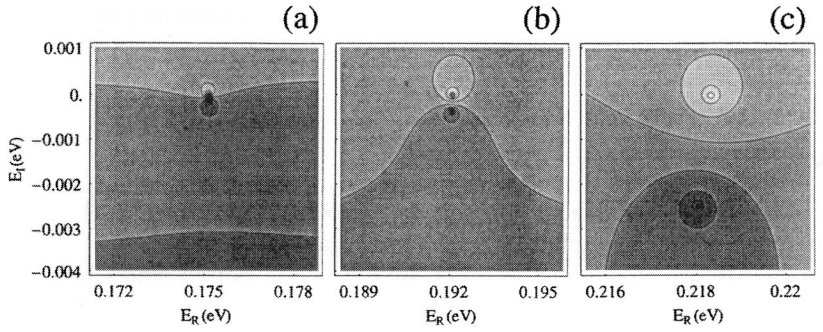

Fig. 4. Contour plots of the pole-zero pairs in the complex energy plane of the S-matrix for $D = 200$ Å near resonances (a) $E = 0.17487$ eV, (b) $E = 0.19196$ eV, and (c) $E = 0.21836$ eV.

of the transmission zero profile. Fig. 4 shows another view of the plots in Fig. 3. The fact that the poles in the complex energy plane are accompanied by zeros on the real axis was shown in ref. 22 to be a result of the unitarity of the S-matrix.

In the neighborhood of the transmission zero, the transmission probability, $|T_{11}(E)|^2$, varies approximately as

$$|T_{11}(E)|^2 \sim \frac{(E-E_R)^2}{(E-E_R)^2+(\gamma)^2} \tag{4.1}$$

and the reflection probability, $|R_{11}(E)|^2 = 1 - |T_{11}(E)|^2$, varies approximately as

$$|R_{11}(E)|^2 \sim \frac{\gamma^2}{(E-E_R)^2+(\gamma)^2} \tag{4.2}$$

These formulas ignore the slight displacement of the position of the pole relative to that of the transmission zero along the real axis. For the transmission zero at $E_f = 0.17487$ eV, $\gamma = 0.0001356$ eV. For the transmission zero at $E_f = 0.19196$ eV, $\gamma = 0.0004639$ eV. For the transmission zero at $E_f = 0.21836$ eV, $\gamma = 0.00333$ eV. We see that both the transmission zero and its accompanying pole are consequences of the Lorentzian form of the reflection probability. We should note that a slight displacement of the position of the pole from the transmission zero along the real energy axis indicates that there are small corrections to the Lorentzian shape of the reflection probability.[24]

Poles of the type shown above, have been observed before in numerical simulations of the waveguide devices. They have been seen in the

double-barrier resonant-tunneling system,[25] for a quantum wire with one side arm,[22, 26] and in a waveguide with an oscillating potential and in a waveguide having an impurity.[21]

IV.2. Bound States

Bound states of the waveguide can also be found using the boundary integral method, by excluding all the propagating modes, and just allowing the evanescent modes in the leads. In Fig. 2, the bound states below the continuum of the first channel found in this manner are marked as arrows. Each bound state of the waveguide that we have found (except for one case discussed below) appears to correspond to a bound state of the closed cavity although the energies are slightly displaced. These trends are clear from the plots of the wavefunctions of the bound states. Figs. 5(a–c) show the probability density of the wavefunctions of the bound states below the first channel in the straight waveguide for cavity widths D = 120 Å,

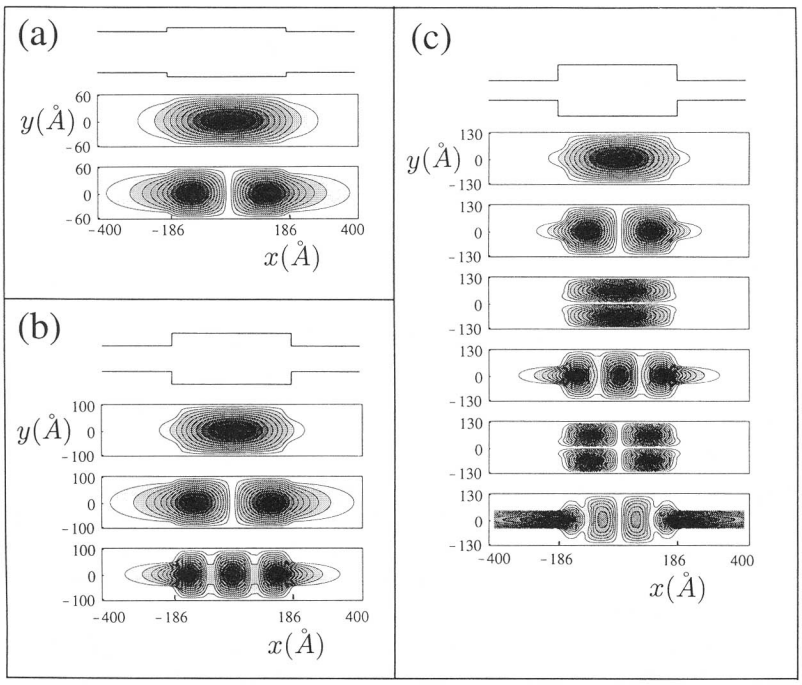

Fig. 5. Probability density of the wavefunctions of the bound states for the open waveguide with $W = 100$ Å, $L = 371.66$ Å, and (a) $D = 120$ Å, (b) $D = 200$ Å, and (c) $D = 260$ Å. The corresponding waveguide dimensions are depicted on top of each plot.

D = 200 Å, and D = 260 Å. The sixth state for D = 260 Å (the exception noted above) occurs just below the continuum and its probability decays but extends far down the lead (about 1000 Å).

The existence of bound states in two-dimensional quantum waveguides was pointed out by Schult *et. al.*[27] who found bound states in a waveguide composed of crossed wires. Also, it is known that the bulges,[28] or the bends or the twisted structues[29] in a waveguide have at least one bound state. The resonance poles below the threshholds of the higher transverse modes in a smoothly varying tube have been found using a perturbation theory.[30]

V. SURVIVAL PROBABILITIES

In this section we will again compute the lifetimes of the quasibound states, but instead of computing the poles of the transmission probability, we will compute survival probabilities which are directly related to the energy Green's function for the waveguide. We will compute the survival probabilities of the three quasibound states in Figs. 3 and 4 since we have obtained decay rates for them from the contour plots. Fig. 6(a) and 6(b) show the transmission probability and the amount of charge in the cavity for energy range including the first three transmission zeros in Fig. 2(b). It is interesting to note that the widths of the transmission zeros and the lifetimes of the quasibound states appear to be correlated to the amount of charge a cavity can hold. This is shown in Fig. 6(b), where we plot the "charge," which is defined in Section III, in the cavity of the infinite waveguide as a function of electron energy. The units are arbitrary because we are plotting the amount of charge in the cavity at one energy relative to the amount at another energy. We see that the charge accumulation around the narrow transmission zeros has extremely high values compared to that for the broad transmission zeros.

Let us now compute the survival probability, $P_\psi(t)$, for an electron placed in the cavity in a quasibound state. The survival probability can be written, $P_\psi(t) = |A_\psi(t)|^2$, where $A_\psi(t)$ is the survival amplitude,

$$A_\psi(t) = \langle \psi | \, e^{-i\hat{H}t/\hbar} \, | \psi \rangle = \int_0^\infty dE \, |\langle \psi \mid E \rangle|^2 \, e^{-iEt/\hbar} \tag{5.1}$$

of an electron placed in the *waveguide cavity* with the same probability amplitude that the electron has at a transmission zero, except that we take only the part inside the cavity and normalize it to one. Thus our initial state, ψ, has no probability outside the cavity. If we know the spectrum of the energy Green's function, $G^+(z) = (z - \hat{H}/\hbar)^{-1}$, where z is a complex

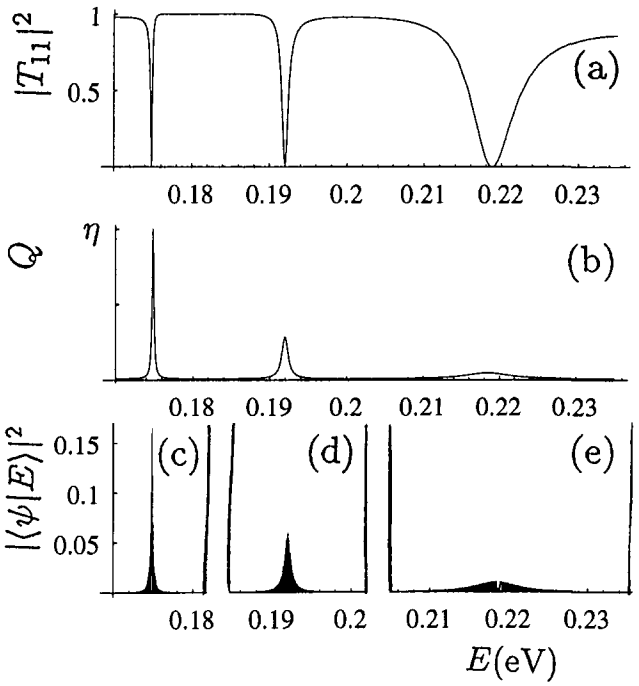

Fig. 6. (a) Transmission probability, $|T_{11}|^2$, versus energy, E, for the open waveguide with $W = 100$ Å, $D = 200$ Å and $L = 371.66$ Å. (b) The charge in the cavity of the open waveguide as a function of energy in arbitrary units. (A "closed" waveguide with lead length, $\Lambda = 2 \times 10^5$ Å, has a similar distribution, but with $\eta = 0.15$.) (c) The spectral density when ψ is the probability amplitude in the waveguide cavity at resonance, $E = 0.17487$ eV. (d) The spectral density when ψ is the probability amplitude in the waveguide cavity at resonance, $E = 0.19196$ eV. (e) The spectral density when ψ is the probability amplitude in the waveguide cavity at resonance, $E = 0.21836$ eV.

number, then the survival probability can be computed from the contour integration,[31] $A_\psi(t) = \int dz\, e^{-izt} \langle\psi|\, G^+(z)\, |\psi\rangle$. Since we do not know the spectrum of the energy Green's function, we shall probe for information about it using Eq. (5.1).

We will use a numerical method which proved successful in computing survival probabilities[32] and resonances[35] for a system with continuous spectrum in an unrelated problem. With this method, one finds the energy eigenstates for a closed finite version of the system consisting of a rectangular cavity (like those in our waveguides) with two very long "leads" of length, Λ, which are closed at the ends. These energy eigenstates can be found using a modified form of the boundary integral method described in Section III. The energy eigenstates of the finite system

can then be used to determine the time dependence of the survival probability, at least for a finite length of time. The length of time, τ_{Δ}, over which the finite system mimics the system with continuous spectrum is $\tau_{\Delta} \approx (\Delta E/\hbar)^{-1}$, where ΔE is the average spacing between energy levels. As we make Λ larger, the energy level spacing will become smaller, and it will take the system a longer time to realize that the "leads" have a finite length. For "lead" length, $\Lambda = 2.0 \times 10^5$ Å, $\tau_{\Delta} \approx 1.4 \times 10^{-11}$ sec (to obtain this number we have used the average spacing of our energy eigenvalues for the closed waveguide with this "lead" length). Also, if the lifetime of the electron is shorter than the time it takes the electron to reach the end of the "lead", the finite system can yield good estimates of decay times. For "lead" length, $\Lambda = 2.0 \times 10^5$ Å, the time it takes an electron, with the Fermi velocity, to travel from the cavity to the end of the 'lead' and back is 4×10^{-11} sec.

In Figs. 6(c–e), we show the spectral density of the initial state, $|\langle \psi \mid E \rangle|^2$, as a function of energy for three different initial states, ψ, namely those three waveguide cavity states associated with the transmission zeros in Fig. 6(a). Notice the strong correlation between the width of the envelope of the spectral density and the width of the transmission zero. The envelope of the spectral density appears to be well represented by a Lorentzian

$$|\langle \psi \mid E \rangle|^2 \approx \frac{(\gamma/\pi)}{(E - E_0)^2 + \gamma^2} \tag{5.2}$$

where E_0 is the energy of the center of the peak and γ is the half-width of the peak when $|\langle \psi \mid E \rangle|^2 = \frac{1}{2}$. There are also oscillations in the plot. The closed system, whose energy eigenstates we used to compute the spectral density, has a discrete set of even and odd (in the longitudinal direction) energy eigenstates which are almost degenerate. The odd eigenstates have very little probability inside the cavity (due to spatial symmetry) and have almost no overlap with the initial state. The even states can have a large overlap with the initial state. Therefore, the plot of the spectral density oscillates between very small and very large values.

The Lorentzian envelope Eq. (5.2) has poles in the complex plane at energies, $E = E_0 \pm i\gamma$. For such a spectral density, the survival amplitude is $A_{\psi}(t) \approx e^{-iE_0 t/\hbar} e^{-\gamma t/\hbar}$. The survival probability is $P(t) \approx e^{-2\gamma t/\hbar}$. Thus, the width, 2γ, is proportional to the inverse lifetime or decay rate for an electron placed in the cavity in state, ψ, at time, $t = 0$. For an electron in the cavity at resonance energy $E = 0.17487$ eV, the width is $2\gamma = 0.000260$ eV and the lifetime is $\tau = \hbar/2\gamma = 2.4 \times 10^{-12}$ sec. For an electron in the cavity at resonance energy, $E = 0.19196$ eV, the width is $2\gamma = 0.000936$ eV and the lifetime is $\tau = \hbar/2\gamma = 6.7 \times 10^{-13}$ sec. For an electron in the cavity at

resonance energy $E = 0.21836$ eV, the width is $2\gamma = 0.00664$ eV and the lifetime is $\tau = \hbar/2\gamma = 0.94 \times 10^{-13}$ sec. We can compare those values to the decay rates we obtained in Section III from the location of the poles on the complex energy plane. For the poles associated with the resonance energy $E = 0.17487$ eV, the distance from the real energy axis is $\gamma = 0.000136$ eV and the lifetime is $\tau = \hbar/2\gamma = 2.4 \times 10^{-12}$ sec. For the poles associated with the resonance energy, $E = 0.19196$ eV, the distance from the real energy axis is $\gamma = 0.000464$ eV and the lifetime is $\tau = \hbar/2\gamma = 7.1 \times 10^{-13}$ sec. For the poles associated with the resonance energy $E = 0.21836$ eV, the distance from the real energy axis is $\gamma = 0.00333$ eV and the lifetime is $\tau = \hbar/2\gamma = 0.99 \times 10^{-13}$ sec. We see that the life times derived from two different methods show good agreement. The decay times that we have obtained, under certain circumstances, can be related to Buttiker's dwell time, which is the average time spent by the particle before it is reflected or transmitted.[33] Buttiker's dwell time is defined $\tau_D = \int_{-\infty}^{\infty} dt \int_{cavity} |\Psi_n(\mathbf{r}, t)|^2 \, d\mathbf{r}$.[34] If we compute τ_D using a state $\Psi_n(\mathbf{r}, t)$ with an initial condition, $\Psi_n(\mathbf{r}, 0)$, which corresponds to a resonant state initially localized in the cavity, then we obtain $\tau_D = 1/2\gamma$ where γ is the lifetime of that resonant state.

We have also considered the closed waveguide with lead length, $\Lambda = 2.0 \times 10^5$ Å, and have plotted the fraction of probability in the cavity for each energy eigenstate. The plot is identical to Fig. 6(b), but with $\eta = 0.15$. Thus an energy eigenstate at the resonance energy, $E = 0.17487$ eV, has 15% of its probability in the cavity, even though the cavity only occupies 0.186% of the area of the closed waveguide. The energy eigenstates of the finite waveguide, near the resonance energy are localized in the cavity.

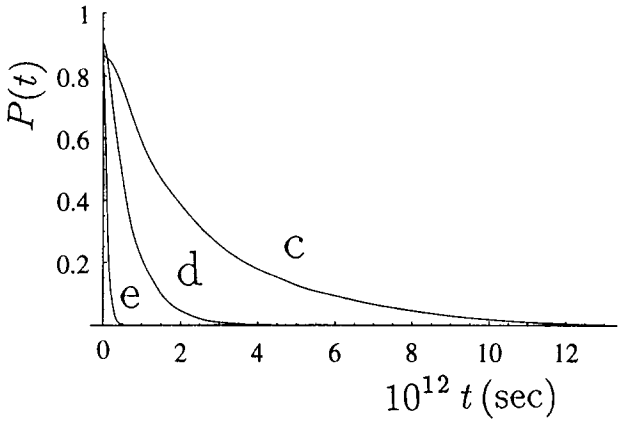

Fig. 7. Survival probabilities for an electron initially localized in waveguide cavity in the waveguide cavity state at (a) $E = 0.17487$ eV, (b) $E = 0.19196$ eV, and (c) $E = 0.21836$ eV.

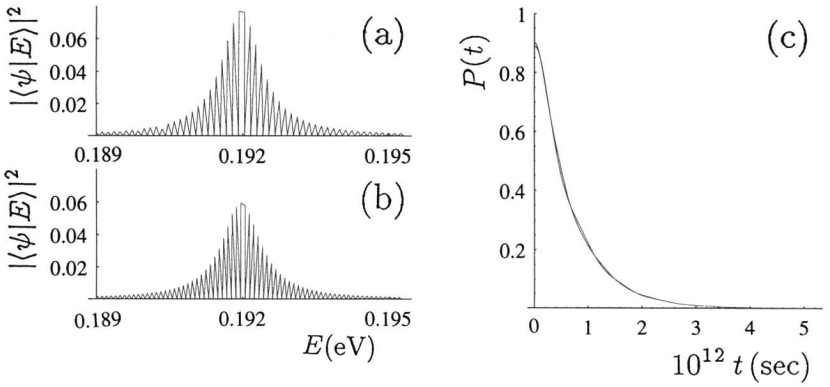

Fig. 8. Spectral density and survival probability when ψ is the probability amplitude in the waveguide cavity at resonance, $E = 0.19196$ eV. (a) Spectral density for lead length, $\Lambda = 1.5 \times 10^5$ Å. (b) Spectral density for lead length, $\Lambda = 2.0 \times 10^5$ Å. (c) Survival probabilities for cases (a) and (b).

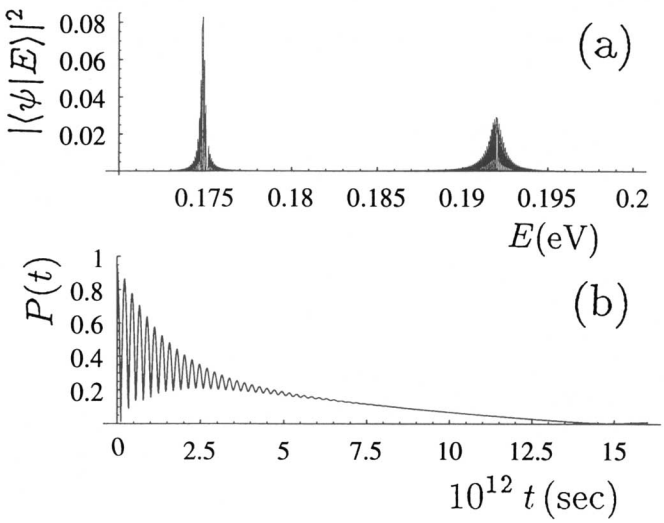

Fig. 9. (a) Spectral density when ψ is a superposition of probability amplitudes of closed cavity eigenstates with eigenenergies at, $E = 0.174671$ eV and $E = 0.191006$ eV. (b) Survival probability from the spectral density in (a).

In Fig. 7, we plot the survival probability, $P(t) = |A(t)|^2$, versus time, t, for each of the the three cases shown in Fig. 6. Our plots of the survival probability show the exponential decay of the electron out of the cavity. The decay rate is determined by the *envelope* of the spectral density. The envelope of the spectral density is fairly insensitive to the average spacing of the energy levels or even whether they are complete, as long as we have enough levels to determine where the envelope lies. The time scale used for the survival probability plots is determined from the period of oscillations in Fig. 9 which we discuss below. What this method does not appear to predict well is the very short time behavior of $P(t)$.

In Fig. 8, we plot the spectral densities and survival probabilities for the resonance at $E = 0.19196$ eV, but using energy eigenstates for closed waveguides with two different lead lengths, $\Lambda = 1.5 \times 10^5$ Å and $\Lambda = 2.0 \times 10^5$ Å. We see that increasing the lead length decreases the spacing of energy eigenstates, but does not affect the envelope of the spectral density, and therefore does not affect the decay rate.

The survival probability can act as a probe of the spectral properties of the system. To show this, we have placed the electron in a state in the cavity which is a superposition of the two neighboring energy eigenstates of the *closed cavity* at energies $E = 0.174671$ eV and $E = 0.191006$ eV. In Fig. 9(a) we show the spectral density, $|\langle \psi \mid E \rangle|^2$, for this initial state. It now has two peaks. The survival amplitude can be written

$$A(t) = \frac{1}{2} \int dE\, e^{iEt} \left(\frac{(\gamma_1/\pi)}{(E-E_1)^2 + \gamma_1^2} + \frac{(\gamma_2/\pi)}{(E-E_2)^2 + \gamma_2^2} \right)$$

$$\approx \frac{1}{2} (e^{-iE_1 t/\hbar} e^{-\gamma_1 t/\hbar} + e^{-iE_2 t/\hbar} e^{-\gamma_2 t/\hbar}) \tag{5.3}$$

The survival probability is

$$P(t) = |A(t)|^2 = \tfrac{1}{4}[e^{-2\gamma_1 t/\hbar} + e^{-2\gamma_2 t/\hbar} + 2\cos((E_1 - E_2)\, t/\hbar)\, e^{-(\gamma_1 + \gamma_2)t/\hbar}] \tag{5.4}$$

Thus if several complex poles contribute to the decay, the survival probability will decay in an oscillatory manner due to interference. We show this in Fig. 9(b).

VI. CONCLUSIONS

Our numerical calculations of the conductance and survival probabilities of electrons in ballistic waveguides indicate that real experiments

on the static conductance of these systems might provide a new way to measure the spectral properties of waveguide cavities. Observed deviations from predicted electron lifetimes in the waveguide cavities may provide a tool for determining the importance of many-body effects and other sources of deviation from ballistic behavior in actual waveguides.

APPENDIX

In this Appendix we show how we obtain the reflection and transmission coefficients. If we require that the wave function be continuous across boundaries of the cavity and apply Green's theorem, we get the matrix equation,[17]

$$\oint d\tilde{l}\left(\Psi_{R,L}(x, y)\frac{\partial\phi_{n'n_o}(x, y)}{\partial\tilde{n}} - \frac{\partial\Psi_{R,L}(x, y)}{\partial\tilde{n}}\phi_{n'n_o}(x, y)\right) = 0 \qquad \text{(A.1)}$$

$\phi_{n'n_o}(x, y)$ is one of the complete set of eigenstates of the Hamiltonian H. In our case these are given by $e^{ik_{n'}x}\chi_{n'}(y)$ or $e^{-ik_{n'}x}\chi_{n'}(y)$. $\tilde{l}$ and $\tilde{n}$ are local coordinates. $\tilde{l}$ measures parallel to the boundary in a counterclockwise direction and $\tilde{n}$ is the outward normal at the boundary. Because the wavefunction vanishes on the top and bottom boundaries, the above equation divides into left and right boundary regions. If we substitute Eq. (3.1), Eq. (3.2), and Eq. (3.6) into equation (A.1), we obtain

$$\begin{aligned}
\sum_{n'=1}^{\infty}\sum_{n=1}^{\infty}\Bigg(\Bigg(&\int_{x=-l} dy\, c_n\chi_n(y)\frac{\partial\phi_{n'n_o}(x, y)}{\partial x} \\
&+\int_{x=-l} dy\, c_n(ik_n)\,\chi_n(y)\,\phi_{n'n_o}(x, y)\Bigg)R_{nn_o} \\
&+\Bigg(\int_{x=l} dy\, c_n\chi_n(y)\frac{\partial\phi_{n'n_o}(x, y)}{\partial x} \\
&-\int_{x=l} dy\, c_n(ik_n)\,\chi_n(y)\,\phi_{n'n_o}(x, y)\Bigg)T_{nn_o} \\
&+\int_{x=-l} dy\, b_n e^{i2\pi n(y+w)/dl}\phi_{n'n_o}(x, y)\,B^{L1}_{nn_0} \\
&+\int_{x=-l} dy\, b_n e^{i2\pi n(y-w)/dl}\phi_{n'n_o}(x, y)\,B^{L2}_{nn_0}
\end{aligned}$$

$$-\int_{x=l} dy\, b_n e^{i2\pi n(y+w)/d1}\phi_{n'n_o}(x, y)\, B^{R1}_{nn_0}$$

$$-\int_{x=l} dy\, b_n e^{i2\pi n(y-w)/d1}\phi_{n'n_o}(x, y)\, B^{R2}_{nn_0}\Bigg)$$

$$= \sum_{n'=1}^{\infty} \int_{x=-l} dy \left(-\frac{1}{\sqrt{k_{n_o}}}\chi_n(y)\frac{\partial \phi_{n'n_o}(x, y)}{\partial x} + ik_{n_o}\chi_{n_o}(y)\,\phi_{n'n_o}(x, y)\right), \tag{A.2}$$

where y is taken from $-w$ to w, $B^{L1}_{nn_0}$ and $B^{L2}_{nn_0}$ are left hard wall coefficients corresponding to the lower and upper segments, and $B^{R1}_{nn_0}$ and $B^{R2}_{nn_0}$ are the corresponding right hard wall coefficients. Eq. (A.2) forms the matrix equation, $A\mathbf{x} = b$, where $\mathbf{x}$ contains the unknown coefficients including R_{nn_o} and T_{nn_o}. The number of modes, n and n' which include both propagating and evanescent modes, determines the size of the matrix. The number of evanescent modes retained is decided by checking the convergence of the electron probability.

To get the coefficient $C_{n'n_o}$ and $C'_{n'n_o}$ we use the fact that the wavefunctions across the cavity boundaries are continuous.

$$\Psi_{R,L}(x, y) = \Psi_C(x, y) \tag{A.3}$$

If we multiply both sides of Eq. (A.3) with the one of the eigenstates, $\phi_{n'n_o}(x, y)$, and integrate around the boundary, we obtain

$$\oint d\tilde{l}\, \Psi_{R,L}(x, y)\,\phi_{n'n_o}(x, y) = \sum_{n'=1}^{\infty} d_{n'}\Bigg(C_{n'n_o}\oint d\tilde{l}\, e^{ik_{n'}x}\chi_{n'}(y)\,\phi_{n'n_o}(x, y)$$

$$+ C'_{n'n_o}\oint d\tilde{l}\, e^{-ik_{n'}x}\chi_{n'}(y)\,\phi_{n'n_o}(x, y)\Bigg) \tag{A.4}$$

From the orthonomality of the eigenstates, $\phi_{n'n_o}$, we can obtain $C_{n'n_o}$ and $C'_{n'n_o}$.

ACKNOWLEDGMENTS

The authors wish to thank the Robert A. Welch Foundation Grant No. F-1051, NSF Grant No. INT-9602971, and DOE Contract No. DE-FG03-94ER14405 for partial support of this work. We thank NPACI and the University of Texas at Austin High Performance Computing Center for

use of their computer facilities. The authors also which to thank Professor German Luna-Acosta for many helpful discussions concerning waveguides, and Professor Alex de Lozanne for helpful discussions concerning experiments.

REFERENCES

1. C. M. Marcus, A. J. Rimberg, R. M. Westervelt, P. F. Hopkins, and A. C. Gossard, *Phys. Rev. Lett.* **69**:506 (1992).
2. M. A. Eriksson, R. G. Beck, M. Topinka, J. A. Katine, R. M. Westervelt, K. L. Campman, and A. C. Gossard, *Appl. Phys. Lett.* **69**:671 (1996).
3. S. Datta, *Electronic Transport in Mesoscopic Systems* (Cambridge University Press, Cambridge, 1995).
4. F. Sols and M. Macucci, *Phys. Rev. B* **41**:11887 (1990); J. Martorell, S. Klarsfeld, D. W. L. Sprung and H. Wu, *Solid State Commun.* **78**:13 (1991); H. Wu, D. W. L. Sprung, and J. Martorell, *Phys. Rev. B* **45**:11960 (1992); Y. B. Gaididei and O. O. Vakhnenko, *J. Phys. Condens. Matter* **6**:3229 (1994); C.-K. Wang and K.-F. Berggren, and Z.-l. Ji, *J. Appl. Phys.* **77**:2564 (1995); K. Lin and R. L. Jaffe, *Phys. Rev. B* **54**:5750 (1996).
5. K. Vacek, A. Okiji, and H. Kasai, *Phys. Rev. B* **47**:3695 (1993); K. Vacek, H. Kasai, and A. Okiji, *J. Phys. Soc. Japan* **61**:27 (1992).
6. A. Okiji, H. Kasai, and A. Nakamura, *Prog. Theor. Phys. Suppl.* **106**:209 (1991).
7. K.-F. Berggren and Z.-l. Ji, *Phys. Rev. B* **43**:4760 (1991).
8. T. Itoh, N. Sano, and A. Yoshii, *Phys. Rev. B* **45**:14131 (1992).
9. C. S. Lent, *Appl. Phys. Lett.* **57**:1678 (1990).
10. Y. Avishai and Y. B. Band, *Phys. Rev. B* **41**:3253 (1990); Y. Avishai, M. Kaveh, and Y. B. Band, *Phys. Rev. B* **42**:5867 (1990); H. U. Baranger, *Phys. Rev. B* **42**:11479 (1990); H. Ishio and K. Nakamura, *J. Phys. Soc. Japan* **61**:2649 (1992); I. Y. Popov, S. L. Popova, *Phys. Lett. A* **173**:484 (1993); P. Exner, P. Seba, M. Tater, and D. Vanek, *J. Math. Phys.* **37**:4867 (1996).
11. C. S. Lent and S. Sivaprakasam, *Proc. Int. Soc. Opt. Eng. SPIE* **1284**:31 (1990).
12. R. Landauer, *Phil. Mag.* **21**:863 (1970); R. Landauer, *J. Phys. Condens. Matter* **1**:8099 (1989); M. Buttiker, *Phys. Rev. Lett.* **57**:1761 (1986).
13. R. Kubo, *Can. J. Phys.* **34**:1274 (1956).
14. D. S. Fisher and P. A. Lee, *Phys. Rev. B* **23**:6851 (1981).
15. H. U. Baranger and A. D. Stone, *Phys. Rev. B* **40**:8169 (1989).
16. G. Garcia-Calderon, A. Rubio, and R. Romo, *J. Appl. Phys.* **69**:3612 (1991).
17. F. R. Frohne, M. J. McLennan, and S. Datta, *J. Appl. Phys.* **66**:2699 (1989).
18. C. M. Marcus, R. M. Westervelt, P. F. Hopkins, and A. C. Gossard, *Chaos* **3**:643 (1993).
19. K. Nakazato and R. J. Blaikie, *J. Phys. Condens. Matter* **3**:5729 (1991).
20. P. F. Bagwell, *Phys. Rev. B* **41**:10354 (1990).
21. P. F. Bagwell and R. K. Lake, *Phys. Rev. B* **46**:15329 (1992).
22. Z. Shao, W. Porod, and C. S. Lent, *Phys. Rev. B* **49**:7453 (1994).
23. U. Fano, *Phys. Rev.* **124**:1866 (1961).
24. F. Schwabl, *Quantum Mechanics* (Springer, New York, 1992).
25. P. J. Price, *Appl. Phys. Lett.* **62**:289 (1993); P. J. Price, *Phys. Rev. B* **48**:17301 (1993).
26. W. Porod, Z. Shao, and C. S. Lent, *Appl. Phys. Lett.* **61**:1350 (1992).
27. R. L. Schult, D. G. Ravenhall, and H. W. Wyld, *Phys. Rev. B* **39**:5476 (1989).
28. M. Andrews and C. M. Savage, *Phys. Rev. A* **50**:4535 (1994); W. Bulla, F. Gesztesy, W. Renger, and B. Simon, *Proc. AMS* **125**:1487 (1997).

29. J. Goldstone and R. L. Jaffe, *Phys. Rev. B* **45**:14100 (1992); J. P. Carini, J. T. Londergan, K. Mullen, and D. P. Murdock, *Phys. Rev. B* **46**:15538 (1992); **48** 4503 (1993); J. P. Carini, J. T. Londergan, D. P. Murdock, D. Trinkle, and C. S. Yung, *Phys. Rev. B* **55**:9842 (1997); J. P. Carini, J. T. Londergan, D. P. Murdock, *Phys. Rev. B* **55**:9852 (1997); P. Exner and P. Seba, *J. Math. Phys.* **30**:2574 (1989).
30. P. Duclos, P. Exner, and P. Stovicek, *Ann, Inst. H. Poincare* **62**:81 (1995).
31. E. N. Economou, *Green's Functions in Mathematical Physics*, (Springer-Verlag, Berlin, 1983).
32. S. Cocke and L. E. Reichl, *Phys. Rev. A* **52**:4515 (1995).
33. M. Buttiker, *Phys. Rev. B* **27**:6178 (1983).
34. G. Iannaccone, *Phys. Rev. B* **51**:4727 (1995); G. Iannaccone and G. Pellegrini, *Phys. Rev. B* **53**:2020 (1996).
35. T. R. Ravuri, V. A. Mandelshtam, and H. S. Taylor, *Superlattices and Microstructures* **20**:87 (1996).